

$\exp(-\hbar\Omega/k_B T)]^{-1}$ . The comparison between Figs. 3B and 3C indicates that this theoretical prediction is in reasonable agreement with the experimental data. However, there are significant differences concerning the line shape that are not understood.

To further support our interpretation, as well as to provide a quantitative estimate of the variance  $\langle Q^2 \rangle$ , we obtained the absolute RS cross section by comparing  $\text{KTaO}_3$  with the standard  $\text{CaF}_2$  using the 514.5-nm laser line. From these measurements, if we ignore the dependence of the polarizability on the wave vector, we find that for the  $A_{1g}$  component,  $\mathcal{P}_{11} = \mathcal{P}_{22} = \mathcal{P}_{33} = a = (6 \pm 2) \times 10^{15} \text{ cm/g}$ , which compares favorably with the value  $a = (4 \pm 1) \times 10^{15} \text{ cm/g}$  that we obtain from the pump-probe experiments using Eqs. 3 and 5. From these values, we determine the proportionality constant relating  $\partial\langle Q^2 \rangle/\partial t$  to  $\Delta\mathcal{T}/\mathcal{T}$ , and from the spontaneous RS measurements (20), we obtain  $\langle Q^2(0) \rangle$ , which corresponds to the standard quantum limit  $\Delta P_q = \Omega\Delta Q_q = (\hbar\Omega/2)^{1/2}$ . Combining these results and integrating  $\Delta\mathcal{T}/\mathcal{T}$ , we get  $\langle Q^2(t) \rangle / \langle Q^2(0) \rangle$ . In Fig. 4, we plot  $\mathcal{S} = 1 - [\langle Q^2(t) \rangle / \langle Q^2(0) \rangle]^{1/2}$ , which is referred to as the squeezing factor (21);  $\mathcal{S}$  corresponds to  $\mathcal{S} > 0$ . We notice that, for  $\xi_{sq} \ll 1$ , Eqs. 3 and 4 predict that  $\mathcal{S} (\ll 1)$  should be proportional to the pump energy density  $I_0$ . This prediction is well obeyed for densities in the range  $I_0 \approx 5$  to  $20 \mu\text{J}/\text{cm}^2$  (Fig. 4, inset).

(9) to provide the basis of bond-polarizability models of intrabranch or overtone ( $\beta$ , 9) second-order RS. We recall that the usually dominant first-order RS is accounted for by an expression that is of the same form as Eq. 1 but is linear in  $Q_q$ , with  $\mathbf{q} \approx 0$  ( $\beta$ , 9). Although the absence of first-order scattering is not required to achieve squeezing, we simplify the discussion by focusing on materials of symmetry such that the linear terms vanish. Also note that, in general,  $\mathcal{P}_\beta$  contains interbranch in addition to the intrabranch contributions shown in Eq. 1. The former have not been included because they are typically much weaker than the terms of interest (9).

- Squeezing relies primarily on the fact that  $U_q$  is proportional to  $Q_q^2$  and not so much on the particular form of the coupling to the field. Squeezing can also be obtained from the term giving two-phonon absorption, that is,  $U_q = \mathbf{F} \cdot \mathbf{q} Q_q^2$ , provided  $fFat \neq 0$  ( $\mathcal{Q}$  is the second-order dipole moment).
- These considerations can be easily generalized to include materials that exhibit first-order RS. However, there is an important distinction in that terms linear in  $Q_q$  generate states with displaced vacua, that is,  $\langle Q_q \rangle \neq 0$ , whereas quadratic contributions do not. Linear terms lead to one-mode coherent states [R. J. Glauber, *Phys. Rev.* **131**, 2766 (1963)], which are the closest to a classical description of the motion.
- Classical squeezing of an oscillator was first demonstrated by D. Rugar and P. Grütter [*Phys. Rev. Lett.* **67**, 699 (1991)]. See also V. Natarajan, F. DiFilippo, D. E. Pritchard, *ibid.* **74**, 2855 (1995).
- Depending on the experimental technique, we expect vacuum squeezing of a solid to manifest itself in different ways. In particular, the neutron or x-ray scattering structure factor is, to lowest order in the field intensity,  $S(\mathbf{k}, t) \approx e^{-2W} [1 - k^2 \langle Q^2(t) \rangle / 2 + \langle Q_q(0)Q_q(t) / M_q \rangle]$ , where  $e^{-2W}$  is the static Debye-Waller factor. Thus,  $S$  contains effects due to both  $\mathbf{k}$ -space (single-mode) and, as in Eq. 4, real-space squeezing.
- Experiments at room temperature reveal behavior that is qualitatively similar to that at 10 K. The 300-K results will be reported elsewhere.
- $\text{KTaO}_3$  crystallizes in the cubic perovskite structure (point group  $O_h$ ) with no first-order Raman active

modes, that is, the leading term in the expansion of the susceptibility is given by Eq. 1. In  $O_h$ , the irreducible Raman representations are  $A_{1g}$ ,  $E_g$ , and  $T_{2g}$ . We singled out the individual contributions by subtracting pairs of spectra obtained with the appropriate choice of polarization directions. Time-domain data were obtained with the polarization of the pump perpendicular to that of the probe beam and oriented along [100] or [010]. In RS, the incident and scattered light were polarized parallel to {110}. Our RS measurements are in good agreement with early experiments reported by W. G. Nielsen and J. G. Skinner [*J. Chem. Phys.* **47**, 1413 (1967)]. The time-domain and RS results reported here are for overtones that transform according to the fully symmetric component  $A_{1g}$ . We find that the behavior of the weaker  $E_g$  spectrum is similar to that of  $A_{1g}$  and that the  $T_{2g}$  contribution is negligible.

- See, for example, L. Dhar, J. A. Rogers, K. A. Nelson, *Chem. Rev.* **94**, 157 (1994); R. Merlin, *Solid State Commun.* **102**, 207 (1997).
- R. Comes and G. Shirane, *Phys. Rev. B* **5**, 1886 (1972).
- The width of the 2TA feature in Fig. 3B is  $0.11 \pm 0.02$  THz. This value gives an upper limit for lifetime effects due to anharmonicity (phonon-phonon interaction).
- We use  $\int \mathcal{S}(\Omega) C^{-1}(\Omega) d\Omega = (2\pi\omega_L^2 \mathcal{E}_L a/c)^2 N M_q^{-1} \langle Q^2(0) \rangle$ , where  $\omega_L$  and  $\mathcal{E}_L$  are the frequency and field of the continuous-wave laser ( $\beta$ ).
- For the variance (Eq. 4), the dominant contributions to the systematic error are the uncertainties in the polarizability (25%) and the integrated intensity of the pulse (20%). The statistical errors in Fig. 4 have been minimized by data averaging and filtering.
- We are indebted to P. Grenier for providing the  $\text{KTaO}_3$  sample and to D. G. Steel for a critical reading of the manuscript. A.K.S. would like to thank the Department of Physics at the University of Michigan for warm hospitality. Supported by the NSF through the Center for Ultrafast Optical Science under grant STC PHY 8920108 and by the U.S. Army Research Office under contract DAAH04-96-1-0183.

2 December 1996; accepted 30 January 1997

## REFERENCES AND NOTES

- R. E. Slusher *et al.*, *Phys. Rev. Lett.* **55**, 2409 (1985); L. Wu *et al.*, *ibid.* **57**, 2520 (1986); D. F. Walls, *Nature* **324**, 210 (1986). See also the special issues on squeezed states; H. J. Kimble and D. F. Walls, Eds., *J. Opt. Soc. Am. B* **4** (no. 10) (1987); E. Giacobino and C. Fabre, Eds., *Appl. Phys. B* **55** (no. 3) (1992).
- J. Janszky and Y. Y. Yushin, *Opt. Commun.* **59**, 151 (1986); J. Janszky and An. V. Vinogradov, *Phys. Rev. Lett.* **64**, 2771 (1990); J. Janszky, P. Adam, An. V. Vinogradov, T. Kobayashi, *Spectrochim. Acta A* **48**, 31 (1992).
- X. Hu and F. Nori, *Phys. Rev. Lett.* **76**, 2294 (1996); X. Hu, thesis, University of Michigan (1996).
- M. Antoni and J. L. Birman, *Phys. Rev. B* **44**, 3736 (1991); *Opt. Commun.* **104**, 319 (1994); X. Hu and F. Nori, *Phys. Rev. B* **53**, 2419 (1996).
- See, for example, C. F. Lo, E. Manousakis, R. Solli, Y. L. Wang, *Phys. Rev. B* **50**, 418 (1994); M. Sonnek and M. Wagner, *ibid.* **53**, 3190 (1996).
- The generation of nonclassical states has been recently demonstrated for a trapped atom by D. M. Meekhof, C. Monroe, B. E. King, W. M. Itano, and D. J. Wineland [*Phys. Rev. Lett.* **76**, 1796 (1996)].
- H. P. Yuen, *Phys. Rev. A* **13**, 2226 (1976); \_\_\_\_\_, and J. H. Shapiro, *Opt. Lett.* **4**, 334 (1979); D. F. Walls and G. J. Wilburn, *Quantum Optics* (Springer, Berlin, 1994), chap. 2.
- M. Born and K. Huang, *Dynamical Theory of Crystal Lattices* (Clarendon, Oxford, 1954), pp. 306–319.
- J. L. Birman, *Theory of Crystal Space Groups and Lattice Dynamics* (Springer, Berlin, 1984), pp. 282–295.
- Such a phenomenological description relying on the Born-Oppenheimer approximation applies strictly only to insulators for which it can be easily formalized

## Tyrosine Phosphorylation of Transmembrane Ligands for Eph Receptors

Katja Brückner, Elena B. Pasquale, Rüdiger Klein\*

Axonal pathfinding in the nervous system is mediated in part by cell-to-cell signaling events involving members of the Eph receptor tyrosine kinase (RTK) family and their membrane-bound ligands. Genetic evidence suggests that transmembrane ligands may transduce signals in the developing embryo. The cytoplasmic domain of the transmembrane ligand Lerk2 became phosphorylated on tyrosine residues after contact with the Nuk/Cek5 receptor ectodomain, which suggests that Lerk2 has receptorlike intrinsic signaling potential. Moreover, Lerk2 is an *in vivo* substrate for the platelet-derived growth factor receptor, which suggests crosstalk between Lerk2 signaling and signaling cascades activated by tyrosine kinases. It is proposed that transmembrane ligands of Eph receptors act not only as conventional RTK ligands but also as receptorlike signaling molecules.

The family of Eph-related receptors can be divided into two subsets based on sequence similarity and on their preference for a sub-

set of ligands that are tethered to the cell surface either by a glycosylphosphatidylinositol (GPI)-anchor or by a single transmembrane domain (1–4). GPI-anchored ligands and their preferred receptors have recently been implicated in establishing topographic projections in the chick retinotectal system and in early patterning events of zebrafish and *Xenopus* brains (5–8). Two Eph receptors, Nuk/Cek5 (9, 10) and Sek4

K. Brückner and R. Klein, European Molecular Biology Laboratory, Meyerhofstrasse 1, 69117 Heidelberg, Germany.  
E. B. Pasquale, The Burnham Institute, 10901 North Torrey Pines Road, La Jolla, CA 92037, USA.

\*To whom correspondence should be addressed. E-mail: Klein@EMBL-Heidelberg.de

(11), that interact with transmembrane ligands (2) have an essential role in the formation of forebrain commissures (12, 13). In contrast to other regions of the embryo (9, 14), in the forebrain, transmembrane ligands are expressed on the axons of commissural neurons and the receptors are expressed in the territories surrounding the pathway followed by commissural axons (12, 13). Moreover, axons that form the anterior commissure are properly guided by catalytically inactive Nuk receptors (12), which suggests that signaling by transmembrane ligands can actively guide these axons in the absence of receptor signaling.

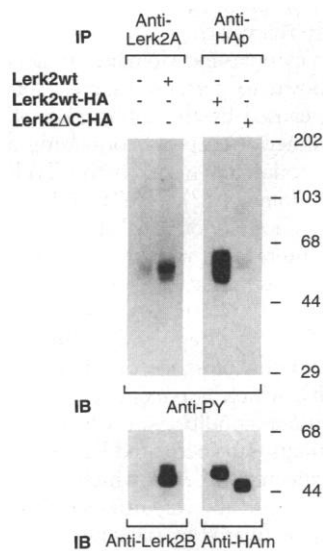
Alignment of the amino acid sequences of the three known transmembrane ligands of Eph receptors, Lerk2/Elk-L, Elf2/HTK-L, and Elk-L3/NLerk2 (1, 15–19), reveals strong sequence conservation of their cytoplasmic domains, including five invariant

tyrosine residues, which suggests interaction with other proteins. Some of these tyrosines are surrounded by amino acid residues that may be recognized as substrates by receptor (20) and nonreceptor tyrosine kinases (21) and could subsequently serve as motifs for phosphotyrosine-binding domains, such as SH2 or PID/PTB domains (22, 23). To test whether Lerk2 is phosphorylated on tyrosine, we expressed wild-type Lerk2 and a truncated form of Lerk2 lacking the cytoplasmic domain (Lerk2 $\Delta$ C) in NIH 3T3 fibroblasts (24). Both an untagged and an epitope-tagged version of wild-type Lerk2, but not Lerk2 $\Delta$ C, were detected by phosphotyrosine-specific antibodies (anti-PY), indicating that in growing cells the conserved tyrosine residues in the cytoplasmic domain are indeed targets for protein tyrosine kinases (PTKs) (Fig. 1).

To investigate whether contact with the receptor Cek5 also regulates phosphorylation of Lerk2, we treated Lerk2-expressing fibroblasts with soluble Cek5 fusion proteins consisting of the Cek5 ectodomain fused to the Fc portion of immunoglobulin G (25). Figure 2A shows that stimulation of Lerk2-expressing fibroblasts with Cek5-Fc,

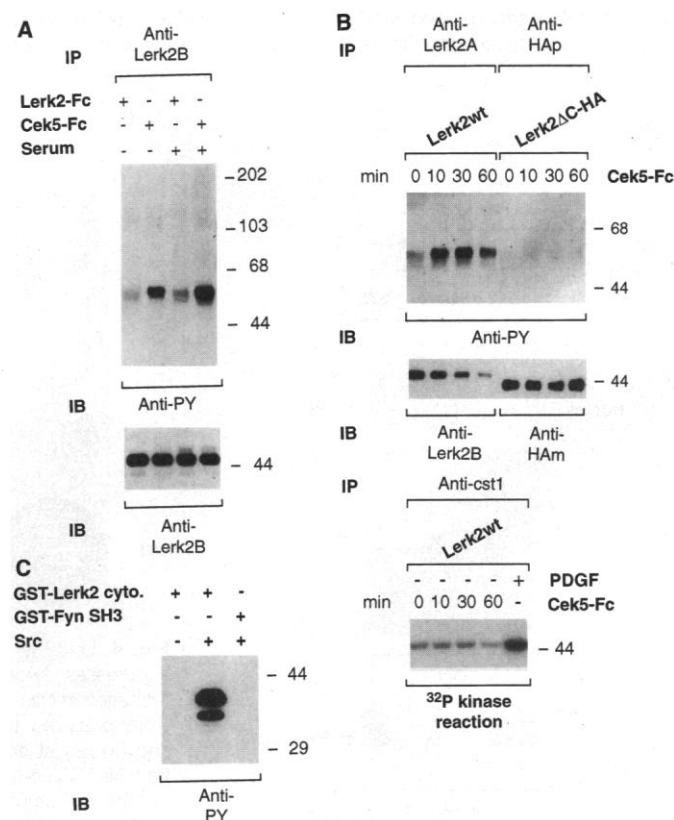
but not with Lerk2-Fc, causes efficient phosphorylation of Lerk2. A time course of Cek5-Fc-induced Lerk2 phosphorylation shows detectable phosphate incorporation after 10 min, with an apparent slow decline after 1 hour (Fig. 2B). However, the amounts of precipitable Lerk2 protein decreased rapidly over the same time period. Because similar losses of Lerk2 protein are observed in immunoblots of total lysates (26), we conclude that Lerk2 is internalized and rapidly degraded. No tyrosine phosphorylation and decrease of Lerk2 protein were observed in cells expressing the truncated Lerk2 $\Delta$ C form, which indicates a requirement for the cytoplasmic domain. Because the Lerk2 cytoplasmic domain does not contain intrinsic kinase activity, Lerk2 phosphorylation must be mediated by a PTK that is endogenous to the ligand-expressing cells. In vitro, the Src tyrosine kinase efficiently phosphorylates the Lerk2 cytoplasmic domain expressed as a glutathione-S-transferase (GST) fusion protein (27) (Fig. 2C). However, kinases of the Src family are not involved in Lerk2 phosphorylation in vivo (Fig. 2B).

In addition, we observed a strong effect



**Fig. 1.** The Lerk2 cytoplasmic domain is tyrosine-phosphorylated when expressed in NIH 3T3 fibroblasts. NIH 3T3 cell lines expressing untagged wild-type Lerk2 (Lerk2wt), epitope-tagged wild-type Lerk2 (Lerk2wt-HA), or epitope-tagged mutant Lerk2 lacking the cytoplasmic domain (Lerk2 $\Delta$ C-HA) were grown to subconfluency, lysed, and immunoprecipitated with antisera against Lerk2 (anti-Lerk2A) or the epitope tag (anti-HAp) (24). Immunoprecipitates (IP) were analyzed by 10% SDS-polyacrylamide gel electrophoresis (SDS-PAGE) and immunoblotted (IB) with monoclonal antibodies to phosphotyrosine (anti-PY). Stripped blots were reprobed with a different Lerk2 antiserum (anti-Lerk2B) or with monoclonal antibodies to HA (anti-HAm) to visualize expression levels. Phosphorylated forms of Lerk2 migrate more slowly than does unphosphorylated Lerk2 and are poorly recognized by immunoblotting with antisera against Lerk2 (bottom panel). The upshift caused by phosphorylation can, however, be observed after longer exposures (see also Fig. 3A). The migration positions of molecular size markers (in kilodaltons) are indicated at right.

**Fig. 2.** Lerk2 phosphorylation is induced by contact with its high-affinity receptor Nuk/Cek5. (A) NIH 3T3 cells expressing Lerk2wt were serum-starved for 24 hours, then either left untreated (–) or incubated for an additional 2 hours in 10% calf serum (+) before stimulation for 10 min with Cek5-Fc or Lerk2-Fc fusion proteins. Immunoprecipitation and immunoblotting were done as described in Fig. 1. (B) NIH 3T3 cells expressing Lerk2wt or Lerk2 $\Delta$ C-HA were incubated with Cek5-Fc (10  $\mu$ g/ml) for the indicated times and subjected to immunoprecipitation and immunoblotting as described above. The amount of precipitable wild-type, but not truncated, Lerk2 decreased rapidly. The same cell lysates were immunoprecipitated with an antibody against the Src family kinases (anti-cst1) (24) and subjected to in vitro kinase assays with the use of [ $\gamma$ - $^{32}$ P]ATP and enolase as substrate. An equal amount of lysate from the same cells treated with PDGF was used as a positive control to detect up-regulation of Src family kinase activity. (C) Src phosphorylates the Lerk2 cytoplasmic domain in vitro. Baculovirus-produced Src protein was immunoprecipitated with antibody 2-17 (anti-Src). Washed precipitates were used in an in vitro kinase reaction with the use of cold ATP with added purified GST fusion proteins (500 ng). Reaction products were analyzed by 10% SDS-PAGE, followed by anti-PY immunoblotting.



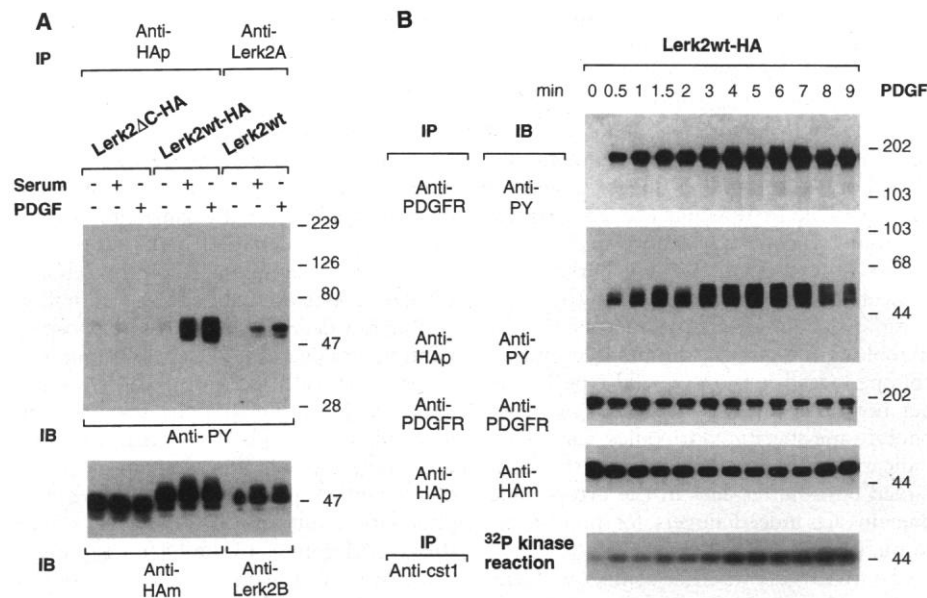


**Fig. 3.** Lerk2 phosphorylation is induced by serum and PDGF. **(A)** NIH 3T3 cells expressing Lerk2wt, Lerk2wt-HA, or Lerk2ΔC-HA were serum-starved for 24 hours, then either left untreated (-) or stimulated (+) with 20% calf serum or PDGF (25 ng/ml) for 10 min. Cell lysates were immunoprecipitated with anti-HAp or anti-Lerk2A and immunoblotted with anti-PY. Stripped blots were reprobed with anti-HAm or anti-Lerk2B as indicated. **(B)** NIH 3T3 cells expressing Lerk2wt-HA were serum-starved for 24 hours, then treated with PDGF (25 ng/ml) for the indicated times. Equal aliquots of the cell lysates were immunoprecipitated with antibodies against either the endogenous PDGF receptor (anti-PDGFR) or anti-HAp to precipitate Lerk2wt-HA, then immunoblotted with anti-PY. A third aliquot of the cell lysates was immunoprecipitated with anti-cst1 and subjected to *in vitro* kinase reactions to detect Src family kinase activity. Stripped blots were reprobed with anti-PDGFR or anti-HAm as indicated. Note the identical kinetics of PDGFR and Lerk2 phosphorylation, in contrast to the delayed activation of Src family kinase activity.

of serum and growth factor stimulation on the phosphorylation of Lerk2 (Fig. 3A), which indicates an additional mechanism for ligand phosphorylation. The rapid kinetics of Lerk2 phosphorylation after stimulation with platelet-derived growth factor (PDGF) (Fig. 3B) suggests that Lerk2 is a direct target of the PDGF receptor tyrosine kinase (RTK). Although a nonreceptor tyrosine kinase, such as Src, may mediate Lerk2 phosphorylation, the slower kinetics of activation of Src family kinases (half-maximal at 3 to 4 min) argues against this (Fig. 3B).

Phosphorylated forms of the Nuk/Cek5 receptor are associated with axonal growth during embryogenesis (28). We found that, correlating with receptor phosphorylation, Lerk2 is tyrosine-phosphorylated in the developing embryo, both in the head and in peripheral sites (Fig. 4A). These results indicate that both receptor and ligand phosphorylation events are physiologically relevant.

The cytoplasmic domain of Lerk2 has been shown to partially suppress focus formation caused by the interaction of Lerk2 with chimeric receptors containing a Nuk/Cek5 ectodomain fused to the TrkB cytoplasmic domain (2). We found that this inhibitory activity of Lerk2 does not depend on the interaction with its high-affinity receptor. Focus formation caused by a number of activated tyrosine kinases, including TrkB, PDGF β receptors, and Src, was suppressed in the presence of wild-type Lerk2 (Fig. 4B), which is tyrosine-phosphorylated under these conditions (26). In contrast, transformation by activated Ras is only marginally affected by Lerk2, which suggests that Lerk2 specifically counteracts signaling pathways activated by tyrosine kinases.

The transmembrane ligands of Eph receptors thus play a dual role: As RTK ligands, they activate signaling pathways in receptor-expressing cells; in addition, their cytoplasmic domains become tyrosine-phosphorylated, allowing interactions with other proteins that may activate signaling pathways in ligand-expressing cells.

The Eph receptor ligand Lerk2 becomes phosphorylated on tyrosine residues by two mechanisms. The first requires interaction with its high-affinity receptor Nuk/Cek5, a finding that was also recently reported by others (29). The identity of the responsible cytoplasmic tyrosine kinase endogenous to the ligand-expressing cell is presently not known. Second, Lerk2 phosphorylation is induced independently of Eph receptor contact by stimulation with peptide growth factors, such as PDGF, that signal through RTKs. In the case of the PDGF receptor, this phosphorylation may be direct and may not involve associated Src family kinases.

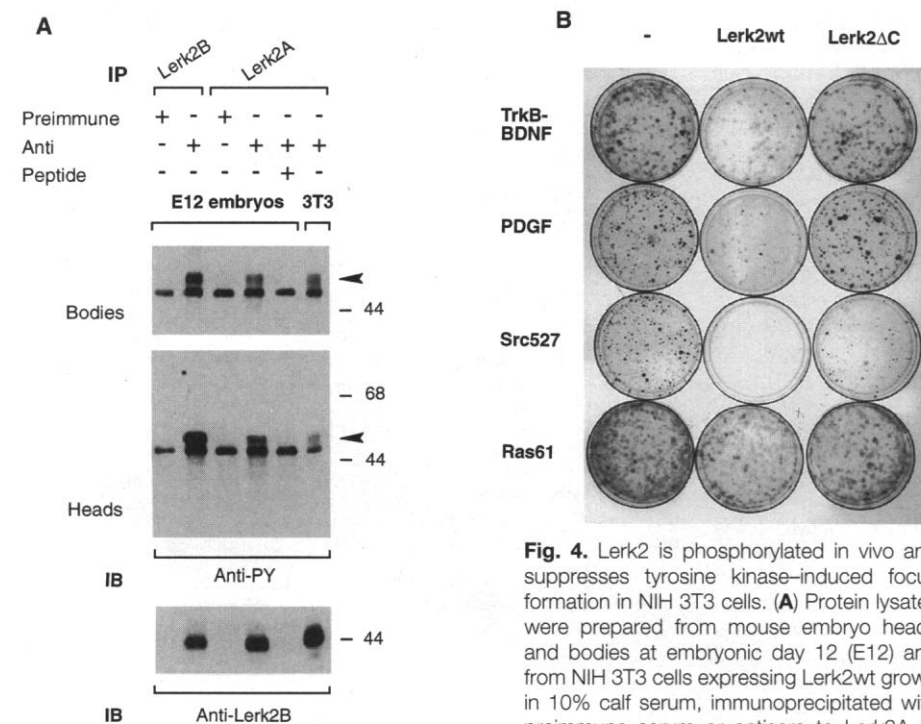


**Fig. 4.** Lerk2 is phosphorylated *in vivo* and suppresses tyrosine kinase-induced focus formation in NIH 3T3 cells. **(A)** Protein lysates were prepared from mouse embryo heads and bodies at embryonic day 12 (E12) and from NIH 3T3 cells expressing Lerk2wt grown in 10% calf serum, immunoprecipitated with preimmune serum or antisera to Lerk2A or Lerk2B, and immunoblotted with anti-PY. Stripped blots were reprobed with antibodies to Lerk2B. *In vivo*-phosphorylated Lerk2 is indicated by arrowheads. The Lerk2 band is competed with the immunizing peptide. **(B)** Focus formation in NIH 3T3 cells (35) induced by cotransfection of expression plasmids encoding BDNF and TrkB, PDGF B-B (causing activation of endogenous PDGF β receptors), or activated forms of Src or H-Ras, in the presence of vector control (-), Lerk2wt, or Lerk2ΔC.

Stripped blots were reprobed with antibodies to Lerk2B. *In vivo*-phosphorylated Lerk2 is indicated by arrowheads. The Lerk2 band is competed with the immunizing peptide. **(B)** Focus formation in NIH 3T3 cells (35) induced by cotransfection of expression plasmids encoding BDNF and TrkB, PDGF B-B (causing activation of endogenous PDGF β receptors), or activated forms of Src or H-Ras, in the presence of vector control (-), Lerk2wt, or Lerk2ΔC.

PDGF may be a physiological inducer of Lerk2 phosphorylation, because many types of central nervous system neurons express PDGF  $\beta$  receptors and respond to PDGF, including neurons of the cerebral cortex, which are known to express Lerk2 (13, 30).

The suppression of mitogenic signaling by Lerk2 may be part of a negative feedback loop, which would reduce the cell's responsiveness to peptide growth factors. Possible mechanisms of action may involve the recruitment of cytoplasmic phosphotyrosine phosphatases (31), which could antagonize signaling pathways downstream of RTKs, or of cytoplasmic tyrosine kinases such as Abl, which mediates growth inhibitory effects by interacting with the cell cycle machinery (32) and is implicated in axonal pathfinding (33). Whatever the mechanism, the discovery of regulated tyrosine phosphorylation of ligands for Eph receptors will rapidly advance our understanding of axonal guidance and possibly of cell growth in the developing embryo.

#### REFERENCES AND NOTES

- S. Davis *et al.*, *Science* **266**, 816 (1994).
- R. Brambilla *et al.*, *EMBO J.* **14**, 3116 (1995).
- R. Brambilla and R. Klein, *Mol. Cell. Neurosci.* **6**, 487 (1995).
- N. W. Gale *et al.*, *Neuron* **17**, 9 (1996).
- U. Drescher *et al.*, *Cell* **82**, 359 (1995).
- H.-J. Cheng, M. Nakamoto, A. D. Bergemann, J. G. Flanagan, *ibid.*, p. 371.
- Q. Xu, G. Aldus, R. Macdonald, D. G. Wilkinson, N. Holder, *Nature* **381**, 319 (1996).
- M. Nakamoto *et al.*, *Cell* **86**, 755 (1996).
- M. Henkemeyer *et al.*, *Oncogene* **9**, 1001 (1994).
- E. B. Pasquale, *Cell Regul.* **2**, 523 (1991).
- N. Becker *et al.*, *Mech. Dev.* **47**, 3 (1994).
- M. Henkemeyer *et al.*, *Cell* **86**, 35 (1996).
- D. Orioli, M. Henkemeyer, G. Lemke, R. Klein, T. Pawson, *EMBO J.* **15**, 6035 (1996).
- J. A. Holash and E. B. Pasquale, *Dev. Biol.* **172**, 683 (1995).
- M. P. Beckmann *et al.*, *EMBO J.* **13**, 3757 (1994).
- B. D. Bennett *et al.*, *Proc. Natl. Acad. Sci. U.S.A.* **92**, 1866 (1995).
- A. D. Bergemann, H.-J. Cheng, R. Brambilla, R. Klein, J. G. Flanagan, *Mol. Cell. Biol.* **15**, 4921 (1995).
- N. A. Nicola *et al.*, *Growth Factors* **13**, 141 (1996).
- N. W. Gale *et al.*, *Oncogene* **13**, 1343 (1996).
- Z. Songyang and L. C. Cantley, *Trends Biochem. Sci.* **20**, 470 (1995).
- N. Stahl *et al.*, *Science* **267**, 1349 (1995).
- P. Bork and B. Margolis, *Cell* **80**, 693 (1995).
- T. Pawson, *Nature* **373**, 573 (1995).
- Generation and culture of NIH 3T3-derived cell lines were done as described (2). For immunoprecipitation analysis, cells were washed twice with phosphate-buffered saline and lysed in Triton-LB [50 mM tris (pH 7.5), 1% Triton X-100, 50 mM NaCl, and 50 mM NaF] with protease inhibitors (Complete, Boehringer), pepstatin, and 0.1 mM sodium orthovanadate. For tissue lysis, 0.5 mM sodium orthovanadate, 10 mM disodium b-glycerophosphate, and 20 mM disodium p-nitrophenylphosphate (Sigma) were additionally included. Polyclonal antiserum to Lerk2A (anti-Lerk2A) was raised against the following COOH-terminal Lerk2 peptide: NH<sub>2</sub>-HYEKVSGDYGHPVY-COOH (34). Polyclonal anti-Lerk2B was raised against a GST-Lerk2 cytoplasmic domain fusion protein (GST-Lerk2 cyto.) expressed in bacteria and purified by glutathione Sepharose (Pharmacia) affinity chromatography. Additional polyclonal antisera included anti-HAp against the hemagglutinin tag

- (HA.11, Babco), anti-PDGF receptor (anti-PDGFR), and anti-cst1 against Src family kinases (from S. Courtneidge and G. Alonso). Mouse monoclonal antibodies included anti-HAm against the hemagglutinin tag (12CA5, Boehringer); anti-PY against phosphotyrosine (4G10, UBI); and 2-17, specific for Src (from S. Courtneidge and P. Lock).
- Cek5-Fc and Lerk2-Fc fusion proteins (from Y. Whang-Zhu) were expressed and affinity-purified by Affigel protein A columns as described [H. Shao *et al.*, *J. Biol. Chem.* **269**, 26606 (1994)].
- K. Brückner, E. B. Pasquale, R. Klein, data not shown.
- Immunoprecipitates were subjected to kinase assays as described [R. M. Kypta *et al.*, *Cell* **62**, 481 (1990)]. Purified GST fusion proteins or acid-denatured enolase were added as exogenous substrates. The SH3 domain of the Fyn kinase was expressed as GST fusion protein (from P. Lock).
- E. B. Pasquale, R. J. Connor, D. Rocholl, H. Schnürch, W. Risau, *Dev. Biol.* **163**, 491 (1994).
- S. Holland *et al.*, *Nature* **383**, 722 (1996).
- A. Smits *et al.*, *Proc. Natl. Acad. Sci. U.S.A.* **88**, 8159 (1991).
- R. F. Paulson, S. Vesely, K. A. Siminovich, A. Bernstein, *Nature Genet.* **13**, 309 (1996).
- A. Goga *et al.*, *Oncogene* **11**, 791 (1995).

- F. B. Gertler, R. L. Bennett, M. J. Clark, F. M. Hoffmann, *Cell* **58**, 103 (1989).
- Single-letter abbreviations for the amino acid residues are as follows: D, Asp; E, Glu; G, Gly; H, His; K, Lys; P, Pro; S, Ser; V, Val; and Y, Tyr.
- Focus-formation assays on NIH 3T3 cells were done as described [R. Klein *et al.*, *Cell* **66**, 395 (1991)], with the use of the following expression plasmids (the amount of DNA per 10-cm dish is given in brackets): TrkB (pFRK46; 500 ng), BDNF (pLL42; 10 ng), PDGF B-B (pSV7d-PDGF-B1; 5 ng [A. Östmann *et al.*, *J. Biol. Chem.* **268**, 16202 (1988)]), pMEXneo (500 ng), Lerk2wt (pRB29; 500 ng), Lerk2 $\Delta$ C (pRB49; 500 ng) (2); H-Ras<sup>Lev51</sup> (pRB34; 50 ng); and Src<sup>Ph527</sup> (pSGTsrc527; 50 ng [T. Eipel *et al.*, *EMBO J.* **14**, 963 (1995)]).
- We thank S. Courtneidge, P. Lock, G. Alonso, C.-H. Heldin, and Y. Wang-Zhu for reagents; R. Brambilla for cell lines; F. Peverali, A. Nebreda, G. Lemke, and T. Graf for helpful discussions; and G. Superti-Furga, P. Orban, and R. Adams for critically reading the manuscript. K.B. is supported by an EMBL predoctoral fellowship. Supported in part by grants from the Deutsche Forschungsgemeinschaft (KI 948/1-1) and NIH (EY10576).

30 September 1996; accepted 27 January 1997

## Spatially and Functionally Distinct Ca<sup>2+</sup> Stores in Sarcoplasmic and Endoplasmic Reticulum

Vera A. Golovina and Mordecai P. Blaustein\*

The organization of calcium (Ca<sup>2+</sup>) stores in the sarcoplasmic and endoplasmic reticulum (S-ER) is poorly understood. The dynamics of the storage and release of calcium in the S-ER of intact, cultured astrocytes and arterial myocytes were studied with high-resolution imaging methods. The S-ER appeared to be a continuous tubular network; nevertheless, calcium stores in the S-ER were organized into small, spatially distinct compartments that functioned as discrete units. Cyclopiazonic acid (an inhibitor of the calcium pump in the S-ER membrane) and caffeine or ryanodine unloaded different, spatially separate compartments. Heterogeneity of calcium stores was also revealed in cells activated by physiological agonists. These results suggest that cells can generate spatially and temporally distinct calcium signals to control individual calcium-dependent processes.

Activation of most cells evokes diverse and complex responses that depend on mobilization of Ca<sup>2+</sup> from intracellular stores in the sarcoplasmic (in muscle) or endoplasmic reticulum (S-ER) (1). Two types of S-ER Ca<sup>2+</sup> stores have been functionally characterized (1-4) and identified by immunocyto-chemical localization of receptors (5). Release of Ca<sup>2+</sup> from one of the stores requires myo-inositol 1,4,5-trisphosphate (IP<sub>3</sub>) (1). Thapsigargin (TG) (2-4, 6, 7) and cyclopiazonic acid (CPA) (3, 7, 8), irreversible and reversible inhibitors of the Ca<sup>2+</sup> pump in the S-ER membrane, respectively, deplete this IP<sub>3</sub>-sensitive store. Mobilization of Ca<sup>2+</sup> from the IP<sub>3</sub>-insensitive store requires cy-

tosolic Ca<sup>2+</sup> in the micromolar range (9) and can be activated by caffeine (CAF) (10) and either activated or blocked by ryanodine (RY), depending on the concentration (11). In some cells, neither TG nor CPA depletes the CAF- and RY-sensitive Ca<sup>2+</sup> store, suggesting that there is also a TG- and CPA-resistant S-ER Ca<sup>2+</sup> pump (2-4).

The S-ER appears to be a continuous, interconnected network of tubules (12). It remains unclear, however, whether the pharmacologically identified stores are spatially separate (1-4) because the two S-ER Ca<sup>2+</sup> stores have not been directly visualized. To perform dynamic high-resolution imaging studies in intact, primary cultured astrocytes and mesenteric artery (MA) myocytes (13), we loaded intracellular organelles preferentially (14) with the Ca<sup>2+</sup>-sensitive, ratiometric fluorochrome fura2 (Figs. 1 and 2), fura-2/FF

Department of Physiology and Center for Vascular Biology and Hypertension, University of Maryland School of Medicine, Baltimore, MD 21201, USA.

\*To whom correspondence should be addressed.